

# Multiband Antenna for Low-Frequency Radio Telescope

RADIAL ANWAR<sup>1</sup>, NORBAHIAH MISRAN<sup>1,2</sup>, MOHAMMAD TARIQUL ISLAM<sup>2</sup>, &  
GERI GOPIR<sup>2,3</sup>

<sup>1</sup>Department of Electrical, Electronic and System Engineering  
Universiti Kebangsaan Malaysia, Bangi, Selangor, 43600, MALAYSIA

<sup>2</sup>Institute of Space Science (ANGKASA)  
Universiti Kebangsaan Malaysia, Bangi, Selangor, 43600, MALAYSIA

<sup>3</sup>School of Applied Physics  
Universiti Kebangsaan Malaysia, Bangi, Selangor, 43600, MALAYSIA

adi\_astro@yahoo.com, bahiah@vlsi.eng.ukm.my, titareq@yahoo.com, gerigopir@gmail.com

*Abstract:* Radio astronomical instrumentation has become a fascinating field of research in astronomy. In this paper, a design of multiband novel antenna for low-frequency radio telescope is proposed. The multiband has been achieved by combining V-shape half-wavelength dipole, traps and parasitic elements. The low return loss, multiband and maximum gain within the zenith direction is provided by V-shape half-wavelength dipole, traps and parasitic elements respectively. The study showed return loss of about -20 dB, -17 dB and -13.6 dB for three different frequencies with maximum achievable gain of about 10.28 dBi. Measurement result shows that the proposed antenna can work properly and meet well to be used in a transient radio telescope which is operated in the urban centers.

*Key-Words:* Radio Telescope, V-shape Antenna, Trap, Parasitic Element

## 1 Introduction

The science of radio astronomy has expanded enormously since the discovery of cosmic radio waves by Karl G. Jansky in 1932. Many new types of astronomical object have been discovered and investigated by radio astronomical methods, and many important discoveries have been made. Quasars, pulsars, Cosmic Microwave Background (CMB) and many other phenomena were first revealed by radio astronomy. This development has intrigued deep exploration in the field of radio astrophysics, computation and in the radio astronomical instrumentation. Invention in the field of radio astronomy has been used in many other field of research. For example is the application of CLEAN algorithm, which is introduced by Jan Högbom to perform a de-convolution process on images created in radio astronomy [1], in incomplete micro-tremors recordings [2]. The other examples are the detection of cancer at centimeter wavelength (~10 GHz) with modern radiometers and using a method of mini-aperture synthesis (interferometry), and the development of very-low-noise receiver over a large frequency range with noise temperature as low as 1 Kelvin per GHz, with wide applications [3].

There are advantages which can be obtained by observing astronomical objects in radio wavelength. Regions of spaces that are opaque to higher-frequency waves such as light are frequently transparent to radio waves and vice versa [4]. The scattering of waves by particles is strongly related to the size of the particles

compared with the wavelength of the incident radiation. Dust clouds in space obscure many of the most interesting features of our galaxy, for examples are the galactic center region and the regions where stars are born. Such regions, which are vital to astronomy, can be investigated by means of their radio frequency emissions which are received without significant losses caused by the interstellar dust clouds.

The second advantage is that there are physical processes occurring in some stars and galaxies which have high intensity emission in the frequency region. These phenomena can be investigated by radio techniques while the associated optical emission may be too weak to be noticed. The discovery of the fascinating quasi-stellar objects (quasars) and pulsating stars (pulsars) are examples of this. Once discovered and accurately located by radio astronomers, the associated optical object may be detected and so allow a broadly based investigation of the nature of the phenomena.

The third advantage is the transparency of the earth atmosphere to most part of radio spectrum. Radiation from celestial objects has been observed nowadays over the whole electromagnetic spectrum, ranging from the very longest radio waves to the extremely short wave gamma rays. However, the part of this radiation which can pass through the earth atmosphere with little absorption is limited to mainly two frequency bands, the optical and the radio frequency regions. Therefore, ground based observation can be conducted within these two frequency bands.

Low-frequency region has become one part of radio astronomy which is observed by many astronomers. Historically, Jansky discovered the existence of radio emissions from outer space at this region [5]. Grote Reber, who is acknowledged as the Father of Radio Astronomy and the inventor of the first radio telescope which is employing dish antenna and become the prototype of many sophisticated radio telescopes nowadays, also explored this region and produced many radio astronomical data, for example is the sky survey at 160 MHz [6]. However, interest in observations at these frequencies ebbed in the 1980s, mostly due to the superior imaging resolution then possible at higher frequencies [7]. Several factors have contributed to revived interest in low-frequency radio astronomy. In the early 1990s a technique was developed which dramatically improved astronomer's ability to mitigate the effects of the ionosphere in aperture synthesis imaging, allowing resolution on the sub-arcminute scale for the first time [8]. Over the same time frame, cost and technology for receivers and digital signal processing suitable for large beamforming arrays improved dramatically, making it reasonable to consider building arrays much larger than previously attempted. In addition, an increasing number of questions in astrophysics and cosmology have emerged in which low-frequency radio astronomy may play an important or essential role [9].

In the field of instrumentation, antenna has become one of the most explored instruments and have been developed in various manner in order to fulfill the needs of the radio astronomers. Simple wire dipole antenna has been used in many radio telescope systems. Examples of such radio telescope include the 22-MHz narrowband dipole array at Penticton, British Columbia, active during the 1960s [10] and Radio JOVE, developed by NASA [11]. However, as it has inherently narrow impedance bandwidth, the observed frequencies are very limited. To achieve large tuning range, previous telescopes such as UTR-2 [12] and TPT [13] used antenna which have inherently large bandwidth, in the sense that the terminal impedance is nearly constant over a large frequency range. Unfortunately, such antennas (the "fat" dipoles and the conical spirals) are mechanically complex, making them expensive, difficult to construct, and prone to maintenance problems [7].

Recently, new types of antenna have been proposed to be used in a low-frequency radio telescope system. Example of such antenna is the inverted-V antenna with dipole arms constructed from aluminum angle (L-shape) stock [14]. Currently, this type of antenna is employed in the Eight-meter-wavelength Transient Array (ETA) radio telescope at Pisgah Astronomical Research Institute (PARI). The resonant frequency of this antenna is at 38 MHz. Nevertheless, with this antenna, ETA can

be operated to conduct observation at 29 MHz - 47 MHz. Another type of antenna is proposed by Paravastu [15]. It is the Fork Antenna which can be operated at 20 MHz - 80 MHz. These antennas are designed to have a wide bandwidth in order to obtain several channels for observation. However, it is reported that data which are obtained by using these antennas are prone to Radio Frequency Interference (RFI) problem.

One of the challenges of the next generation radio telescope for astronomy is its capacity to cope with the increasing problem of RFI [16]. Due to RFI in radio astronomical observation, radio astronomy observatories are usually sited at great distances from major centers of populations to minimize radio frequency interference from other radio services [17]. Several methods for RFI mitigation have been proposed. Examples of these methods includes the spatial filtering of RFI using reference antenna [18] [19] and the algorithm for time and frequency blanking for RFI mitigation [20]. In [21], methods to analytically calculate the probability of interference caused by multiple sources that are scattered randomly over an area are proposed, while in [22], an algorithm for interference rejection in GPS receiver is developed. However the applicability of these methods for RFI mitigation in radio astronomy has not yet been explored. There is no universal method of RFI mitigation in radio astronomy [23] [24]. In particular, the applicability and the success of certain mitigation procedures depend on a number of factors: the type of radio telescope, the type of observations, and the type of RFI [23]. Therefore, in order to apply the RFI mitigation method, additional instrumentation or algorithm is needed with various manners.

As most of radio telescopes employ antenna with continuous wide bandwidth, RFI mitigation process usually started after the received signal pass through the antenna. In other words, the antenna itself cannot reject or filter the RFI. Therefore, without a sophisticated receiver system, a radio telescope will be suffered with RFI problem. However, if radio telescope is designed to observe only within the protected frequency bands by International Telecommunication Union (ITU) for astronomical purposes, radio astronomical observation is possible to be conducted in the urban centers without additional instruments or algorithm at post-processing stage for FRI mitigation.

In this paper, a design of multiband VHF novel antenna for low-frequency transient radio telescope is proposed. The capability to conduct radio astronomical observation in three frequencies is provided by the proposed antenna. Nevertheless, more operating frequencies can be provided by employing more traps in the antenna. The radio telescope can be used to observe astrophysical phenomena which are suspected to produce single pulses detectable at relatively long

wavelengths, as conducted by ETA [25]. Three operating frequencies provide bigger opportunity to detect these phenomena. Another observation which can be conducted with the proposed radio telescope is the Jupiter, Moon and Solar observation. Surveying for radio galaxies and another distance radio source also can be conducted with the proposed radio telescope. With multiband system, power spectrum of the observed objects can be obtained.

## 2 Antenna Configuration

In VHF region, the assigned frequency bands for astronomical purposes are 37.5 MHz–38.25 MHz, 73.0 MHz–74.6 MHz and 150.05 MHz–153.0 MHz [3]. Therefore, the radio telescope is designed to be operated within these frequency bands. Configuration of the proposed antenna for the radio telescope is shown in Fig. 1. The proposed antenna is a combination of V-shape half-wavelength dipole, trap and parasitic elements, comprising a driven element in V-shape and three parasitic elements as director. The antenna is designed to operate in three frequency bands where the resonant frequencies are determined by employing two pairs of trap in the driven element. Each trap made by using commercial-off-the shelf components, comprising two inductors and one capacitor in order to keep the trap as light as possible, as heavy weight trap may lead the antenna to be bended downward and hence ruin its V-shape. The inductors are arranged in series form and parallel to capacitor, to perform a band-stop filter.

The overall length of the driven element is about 3.364 meters. The feed point in the center of the driven element is about 1.6 meter above ground, while the other ends of the driven element are hanged on the main post about 2.59 meters above ground, resulting a V-shape antenna with angle between the arms of about  $108^\circ$ .

Yagi-Uda antenna concept [26-28] is adopted in the proposed antenna director configuration. The first parasitic element is placed at 2.258 meters above the ground with length of 0.888 meters. This length is equal to 90% of half-wavelength of about 152 MHz. The second and third parasitic elements are placed at 2.962 and 4.324 meters respectively above the ground with equal length of 1.839 meters. This length is equal to 90% of half-wavelength of about 73.4 MHz. The distances of these parasitic elements from feed point are about  $\lambda/3$  of its estimated frequencies. Table one showed the parameters of the proposed antenna.

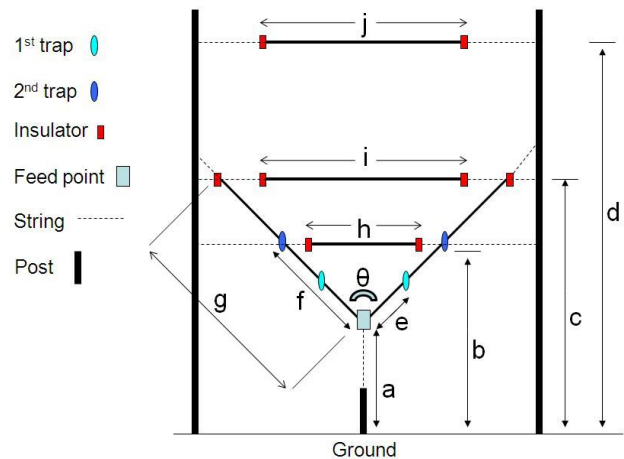


Fig. 1. Diagram of the proposed antenna.

Table 1  
Summary of antenna parameters.

Parameters	Values
Feed point (a)	1.6 m
1 <sup>st</sup> parasitic element (b)	2.258 m
2 <sup>nd</sup> parasitic element (c)	2.962 m
3 <sup>rd</sup> parasitic element (d)	4.324 m
1 <sup>st</sup> trap (e)	0.471 m
2 <sup>nd</sup> trap (f)	0.942 m
Driven element (g)	1.682 m
1 <sup>st</sup> parasitic element length (h)	0.888 m
2 <sup>nd</sup> parasitic element length (i)	1.839 m
3 <sup>rd</sup> parasitic element length (j)	1.839 m
Angle ( $\theta$ )	$108^\circ$

The traps have been simulated using RFSim99. The first pair of trap comprising 61.5 nH and 49 nH inductors, and a 10 pF capacitor to perform a band-stop filter at 151.403 MHz. Fig. 2 shows the diagram of this trap. The trap is placed at each arm of the driven element at distance of 0.471 meters from feed point. At 150.05 MHz–153.0 MHz, the normalized  $|S_{11}|$  parameter of this trap is 1, as shown in Fig. 3, showing that it can work properly to isolate the signal in the driven element between the trap within this frequency band.

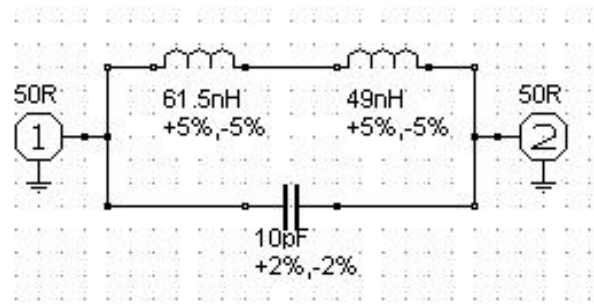


Fig. 2. Diagram of the first trap.

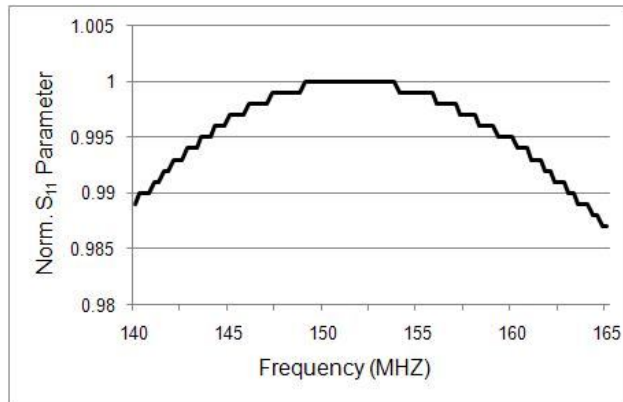


Fig. 3. |S11| parameter of the first trap.

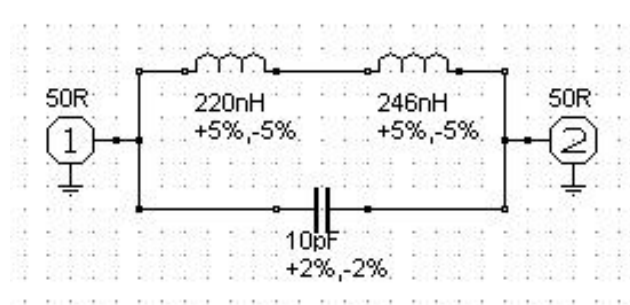


Fig. 4. Diagram of the second trap.

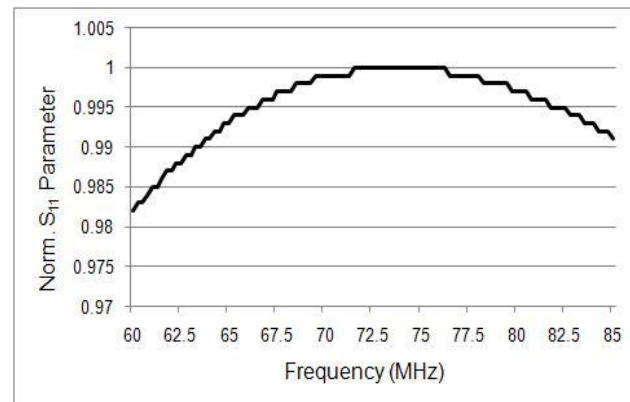


Fig. 5. |S11| parameter of the second trap.

The second pair of trap comprising 220 nH and 246 nH inductors, and a 10 pF capacitor to operate at 73.727 MHz. It is placed at each arm of the driven element at distance of 0.942 meters from feed point. At 73.0 MHz–74.6 MHz, the normalized |S11| parameter of this trap is 1. Fig. 4 and Fig. 5 shows the diagram and plot of |S11| parameter of the second trap respectively.

### 3 Result and Discussion

The parametric studies of the proposed antenna have been analyzed and optimized using numerical electromagnetic code based software (NEC4WIN95). The simulations are conducted with perfect ground parameters. Through a series of simulations of varying the design parameters, the optimized results are obtained for the required return loss and radiation pattern.

Simulated return loss and gain of the proposed antenna are shown in Fig. 6 and Fig. 7 respectively. The return loss  $\leq -10$  dB are obtained at 37.5 MHz – 38.5 MHz, 73.3 MHz – 73.9 MHz and 150.9 MHz – 152 MHz. The study showed that value of inductors within the trap can be used to control the proposed antenna’s resonant frequency at these frequency bands maintaining the return loss less than -10 dB. At 37.5 MHz – 38.5 MHz, return loss peak of about -20 dB is obtained at 38 MHz, with gain variation ranging from 7.56 to 7.47 dBi along the frequency band. Along 73.3 MHz – 73.9 MHz, gain are varies from 8.21 to 8.81 dBi with peak of return loss of about -17 dB at 73.6 MHz. At 150.9 MHz – 152 MHz, peak of the return loss is about -13.6 dB at 151.4 MHz, with gain variation ranging from 9.97 to 10.28 dBi.

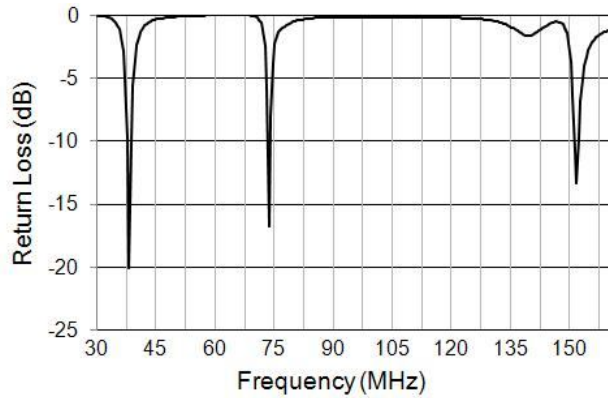


Fig. 6. Simulated return loss of the proposed antenna.

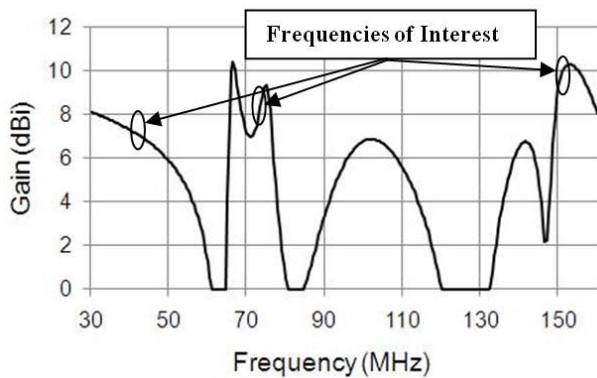


Fig. 7. Simulated gain of the proposed antenna.

The effect on return loss of inductor's value is shown in Fig. 8. The grey dot line shows the return loss of the proposed antenna if the inductor's values within the traps are divided by two, while the dashed-dot line represents the return loss if the inductor's values are multiplied by two. The capacitor's values were adjusted to preserve the operating frequency of each trap.

The study shows that the angle between the arms of the proposed antenna's driven element also can affect the return loss at each operating frequency. Fig. 9 shows the variation on the return loss with different angles of the driven element's arm. Angle of 108° is chosen for the proposed antenna as it provides the most suitable peaks of return loss and bandwidths at each operating frequency relative to the protected bands by ITU.

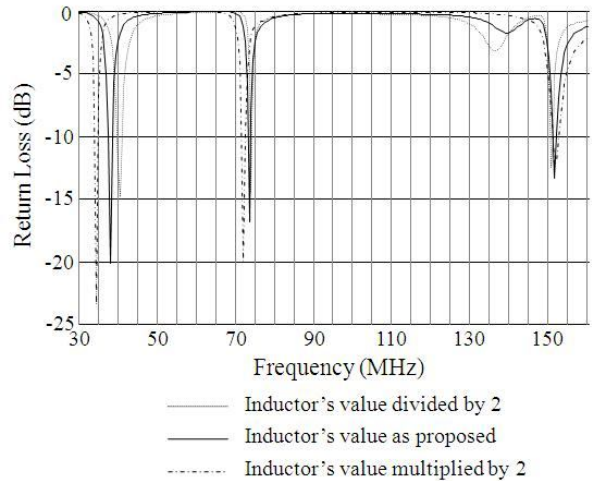


Fig. 8. Effects on return loss of inductor's values within the traps.

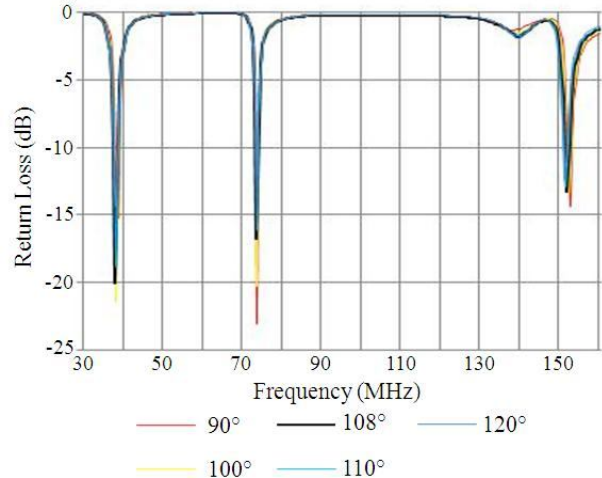


Fig. 9. Effects on return loss of angles between the driven element's arms.

These results are within the protected frequency bands for radio astronomical purposes, except for the first frequency band. A narrow band-pass filter will be used for further limitation of the operating frequencies to ensure that RFI can be avoided. The inductors within the traps also act as coil-loads, resulted the driven element to behave as shortened dipole [29]. Therefore, the length of the driven element is shorter than half-wavelength of the operated frequencies.

Radiation pattern of the proposed antenna has been simulated in the E and H-plane at 38 MHz, 73.6 MHz and 151.4 MHz. At 38 MHz, the maximum gain is about 7.52 dBi with beam-width of 118° at E-plane and 74° at H-plane, as shown in Fig. 10 and Fig. 11 respectively. At 73.6 MHz, the maximum gain is about 8.51 dBi, as shown in Fig. 12 and Fig. 13 respectively. Beam-width at this frequency is 82° at E-plane and 70° at H-plane. At 151.4 MHz the maximum gain is about 10.21 dBi with beam-width of 66° at E-plane and 50° at H-plane. The radiation patterns are shown in Fig. 14 and Fig. 15 respectively. It can be seen that the antenna has almost symmetrical radiation pattern at each simulated frequency. All side-lobes occur in the radiation patterns are below -3dB.

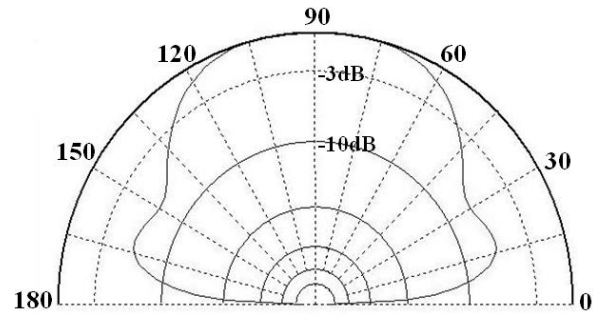


Fig. 12. Far-field E-plane pattern at 73.6 MHz.

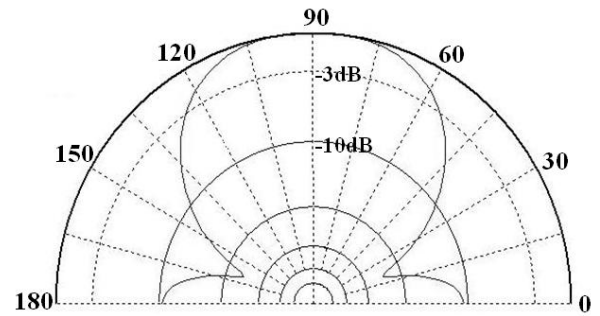


Fig. 13. Far-field H-plane pattern at 73.6 MHz.

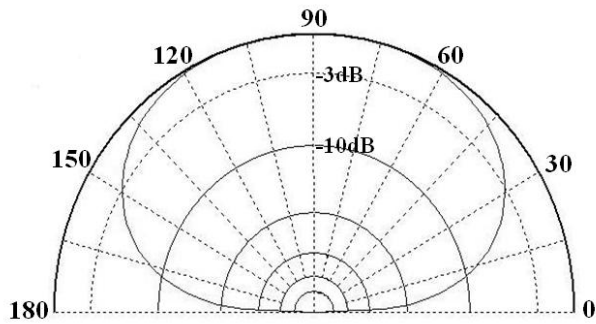


Fig. 10. Far-field E-plane pattern at 38 MHz.

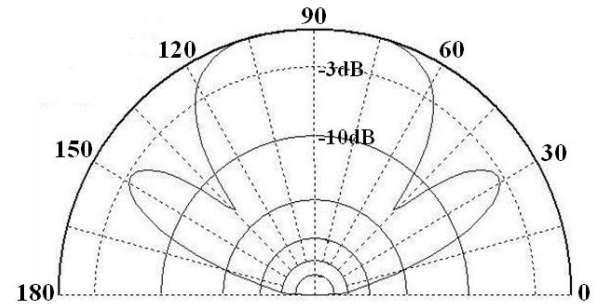


Fig. 14. Far-field E-plane pattern at 151.4 MHz.

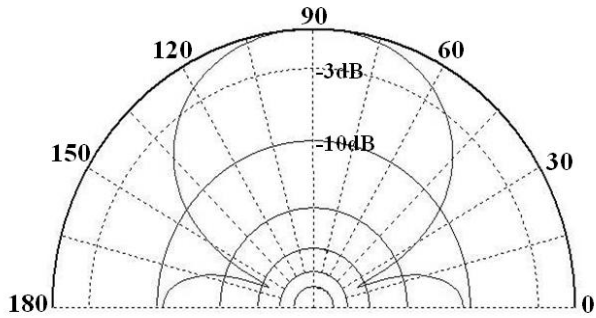


Fig. 11. Far-field H-plane pattern at 38 MHz.

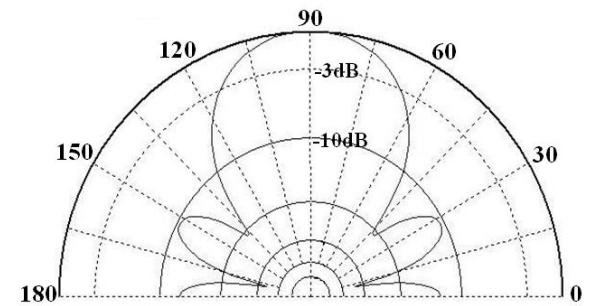


Fig. 15. Far-field H-plane pattern at 151.4 MHz.

In a transient radio telescope, the maximum gain should be achieved at zenith direction. Due to the fix position of the feed point relative to ground measured in unit of wavelength, the direction of the maximum gain of the proposed antenna for the driven element alone will be different for the three operated frequencies. At the middle and highest operated frequencies, maximum gains are not achieved at zenith direction. The parasitic elements as a director are adopted in the proposed design to overcome this shortcoming. These directors provided maximum gain of the antenna within the operated frequencies are in the zenith direction. Fig. 16 and Fig. 17 shows the effect of the parasitic elements to the far-field pattern of the proposed antenna at 73.6 MHz and 151.4 MHz respectively.

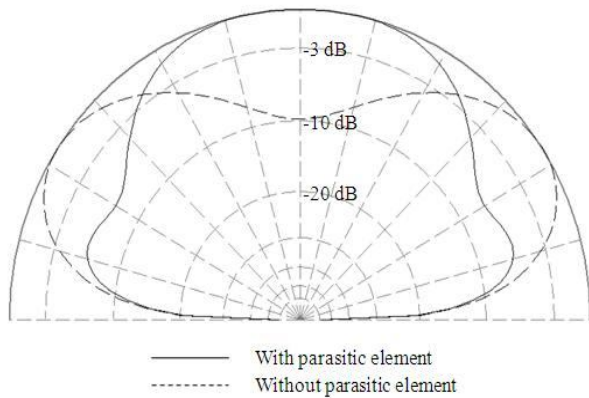


Fig. 16. Effect of the parasitic elements to the far-field pattern at 73.6 MHz.

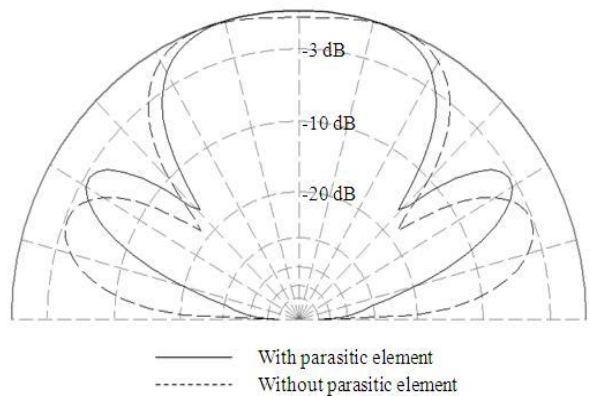


Fig. 17. Effect of the parasitic elements to the far-field pattern at 151.4 MHz.

Another parameter which should be noticed in the proposed antenna design is the height of its feed point relative to the ground. At high frequency (HF) region, the directive properties of any antenna are modified considerably by the ground plane. This is due to the earth that acts as a reflector [30]. If a dipole antenna is placed horizontally above the ground, most of the energy radiated downward from the dipole is reflected upward. The reflected waves combine with the direct waves (those radiated at angles above the horizontal) in various ways, depending on the height of the antenna, the frequency, and the electrical characteristics of the ground under and around the antenna. Due to this characteristic, the radiation pattern of a dipole antenna can be determined from its height from the ground. This characteristic also occurred in the proposed antenna. Feed point's height of about 1.6 meters is chosen as it provides the most suitable radiation pattern of the proposed antenna to be used in a transient radio telescope. The effect of feed point's height to the far-field pattern of the proposed antenna at 73.6 MHz and 151.4 MHz are shown in Fig. 18 and Fig. 19 respectively.

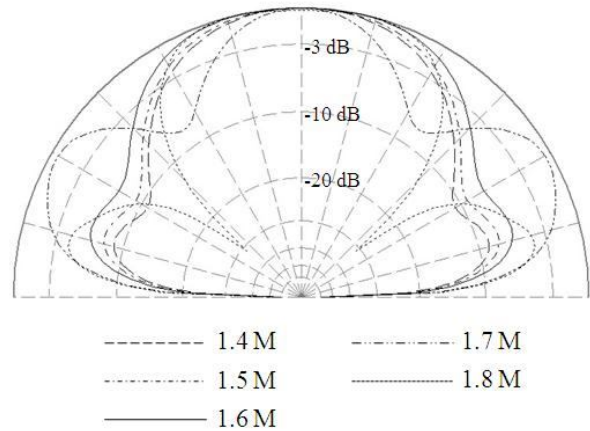


Fig. 18. Effect of height to the far-field pattern at 73.6 MHz.

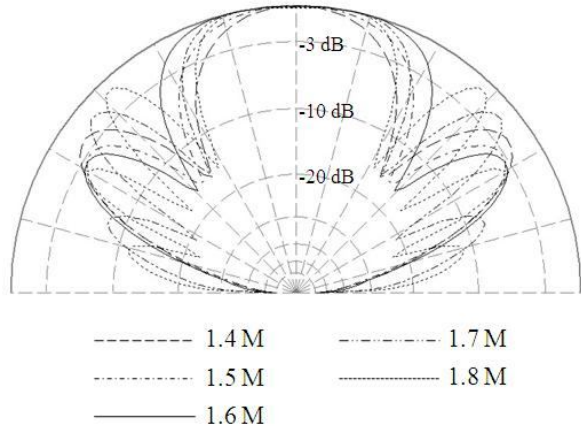


Fig. 19. Effect of height to the far-field pattern at 151.4 MHz.

The proposed antenna was constructed inside the Engineering Faculty of Universiti Kebangsaan Malaysia building for measurement. The antenna was held by strings, as shown in Fig. 20. The reference antenna was placed above the proposed antenna. Power loss which is introduced by the cables was measured. It was observed that total power loss of about 6.4 dB is introduced by the cables. Signals with power of -10 dBm were transmitted at 37.875 MHz, 73.8 MHz, and 151.5 MHz. These frequencies are the frequency centers of the protected bands by ITU for astronomical purposes. The received signals of about -50 dBm at 37.875 MHz and 73.8 MHz, and -60 dBm at 151.5 MHz were observed from a spectrum analyzer, as shown in Fig. 21, Fig. 22 and Fig. 23 respectively.

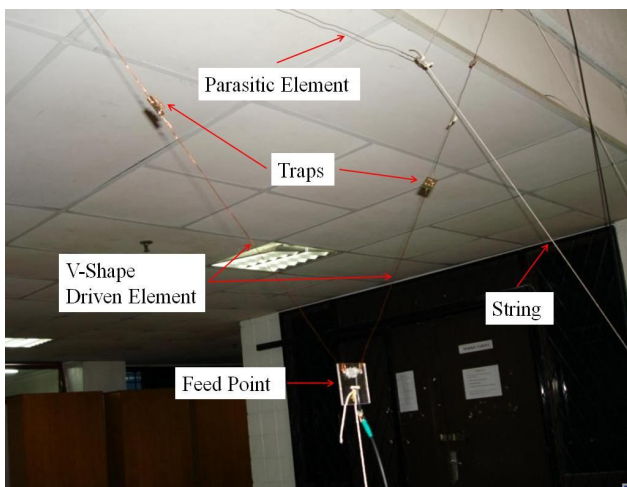


Fig. 20. The constructed antenna.

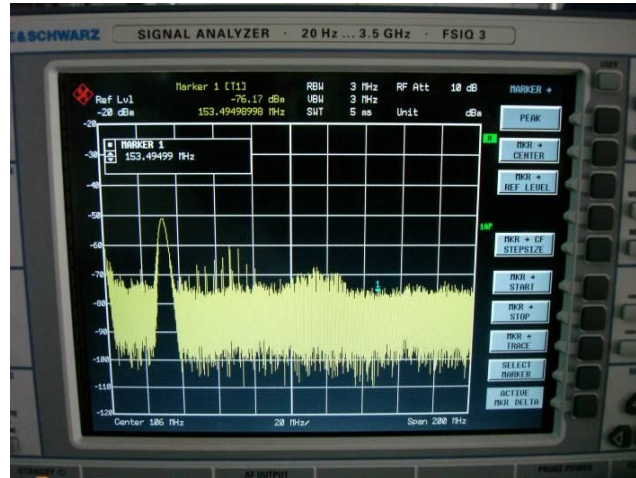


Fig. 21. The received signal at 37.875 MHz.

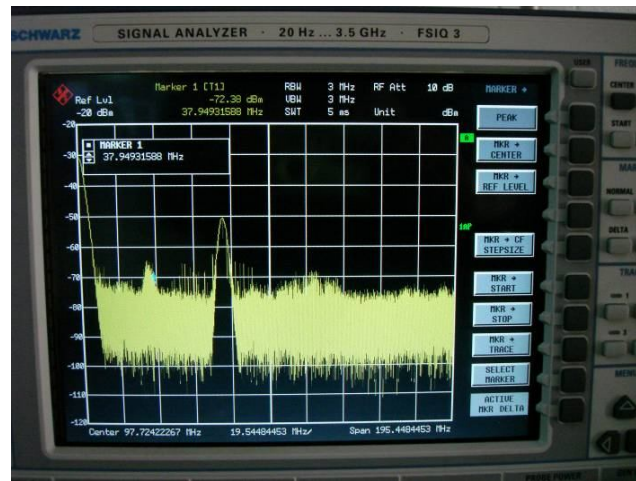


Fig. 22. The received signal at 73.8 MHz.

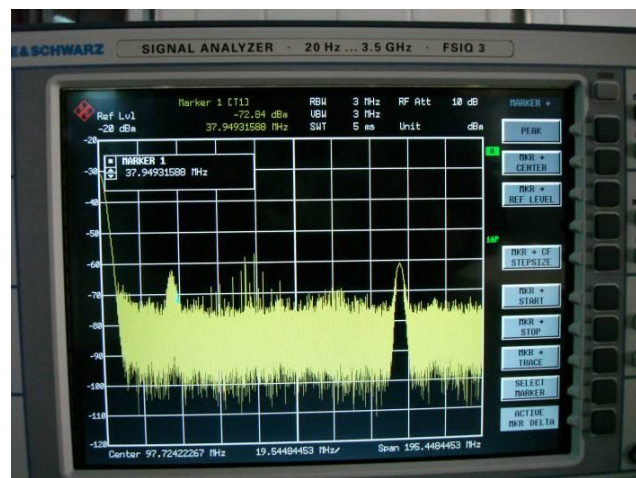


Fig. 23. The received signal at 151.5 MHz.

The measurement result shows that the proposed antenna can work in the designated frequencies. Due to the large geometry of the antenna, it was tested inside the building. This affects the result of the measurement, shown by the low level of the strength of the received signals.

#### 4 Conclusion

A design of multiband antenna for low-frequency radio telescope has been proposed in this paper. The proposed antenna can be operated in three frequencies by using traps, with return loss value down to -20 dB. Nevertheless, the concept which is applied in the proposed antenna can be used to design another antenna with more operating frequencies. Simulation results showed that the proposed antenna has suitable radiation patterns to be used in a transient radio telescope. The radio telescope can be operated in urban centers without additional instrument or algorithm for RFI mitigation.

#### References:

- [1] J. Högbom, Aperture Synthesis with a Non-Regular Distribution of Interferometer Baselines, *Astronomy and Astrophysics Supplement*, Vol. 15, 1974, p.417.
- [2] G. Hloupis, M. Moisiidi, F. Vallianatos, J. Stonham, J. Makris, and D. Triantis, Application of CLEAN Algorithm in Incomplete Microtremors Recordings, *WSEAS Transactions on Circuits and Systems*, Issue 3, Vol. 2, 2003, pp. 557-560.
- [3] CRAF (Committee on Radio Astronomy Frequencies), *CRAF Handbook for Radio Astronomy* 3rd ed., European Science Foundation, 2005.
- [4] W. N. Christiansen, and J. A. Högbom, *Radiotelescope 2<sup>nd</sup>*, Cambridge University Press, 1985.
- [5] K. G. Jansky, Electrical Disturbances Apparently of Extraterrestrial Origin, *Proc. IRE*, Vol. 21, No. 10, 1933, pp. 1387-1398.
- [6] G. Reber, Cosmic Static, *Astrophys. Journal*, Vol. 100, 1944, pp. 279-287.
- [7] S. W. Ellingson, Antennas for the Next Generation of Low-Frequency Radio Telescope, *IEEE Transactions on Antennas and Propagation*, Vol. 53, No. 8, 2005, pp. 2480-2489.
- [8] N. E. Kassim, R. A. Perley, W. C. Erickson, and K. S. Dwarakanath, Subarcminute Resolution Imaging of Radio Sources at 74 MHz With the Very Large Array, *Astronomical Journal*, Vol. 106, 1993, pp. 2218-2228.
- [9] N. E. Kassim and W. C. Erickson, Meter- and Decameter-Wavelength Array for Astrophysics and Solar Radar, *Proc. SPIE*, Vol. 3357, 1998, pp. 740-754.
- [10] C. H. Costian, J. D. Lacey, and R. S. Roger, Large 22-Mhz Array for Radio Astronomy, *IEEE Trans. Antenna Propag.*, Vol. 17, No. 2, 1969, pp. 162-169.
- [11] [Online]. Available: <http://radiojove.gsfc.nasa.gov/>
- [12] S. Ya. Braude et al., Decametric Survey of Discrete Sources in the Northern Sky: I. The UTR-2 Radio Telescope. Experimental Techniques and Data Processing, *Astrophys. Space Sci.*, Vol. 54, 1978, pp. 3-36.
- [13] W. C. Erickson, M. J. Mahoney, and K. Erb, The Clark Lake Teepee-Tee Telescope, *Astrophys. J. Supp. Ser.*, Vol. 50, No. 403, 1982, pp. 403-420.
- [14] S. W. Ellingson, J. H. Simonetti, and C. D. Patterson, Design and Evaluation of an Active Antenna for a 29-47 MHz Radio Telescope Array, *IEEE Transactions on Antennas and Propagation*, Vol. 55, No. 3, 2007, pp. 826-831.
- [15] N. Paravastu, B. Hicks, P. Ray, and W. Erickson, A Candidate Active Antenna Design for a Low Frequency Radio Telescope Array, *Proc. IEEE Int. Antenna and Propagation Symp.*, 2007, pp. 4493-4496.
- [16] A. Fereidontabar, Wide-band Beamformer with Integrated Antenna, *WSEAS Transactions on Communications*, Issue 2, Vol. 8, 2009, pp. 279-289.
- [17] NTIA (National Telecommunications and Information Administration), *Radio Astronomy Spectrum Planning Options*, U.S. Department of Commerce, 1998 [Online]. Available: <http://www.ntia.doc.gov/osmhome/reports/pub9835/raspchp1.htm>
- [18] Van der Veen, A-J. and Boonstra, A-J., Spatial Filtering of RF Interference in Radio Astronomy Using A Reference Antenna, *Proc. IEEE International Conference on Acoustics, Speech, and Signal Processing*, 2004, pp. 189-192.
- [19] B. D. Jeffs, L. Li, and K. F. Warnick, Auxiliary Antenna-Assisted Interference Mitigation for Radio Astronomy Arrays, *IEEE Transactions on Signal Processing*, Vol. 53, No. 2, 2005, pp. 439-451.
- [20] B. Güner, and J. T. Johnson, Time and Frequency Blanking for Radio-Frequency Interference Mitigation in Microwave Radiometry, *IEEE Trans. on Geoscience and Remote Sensing*, Vol. 45, No. 11, 2007, pp. 3672-3679.
- [21] S. Fleurke, A Probability Model for Multiple-Source Interference, *Proc. 12th WSEAS International Conference on Communications*, 2008, pp. 410-415.
- [22] W. L. Mao, Narrowband Interference Rejection in GPS receiver using Adaptive Lattice Predictor, *WSEAS Transactions on Systems*, Issue 2, Vol. 7, 2008, pp. 100-105.

- [23] P. A. Fridman, and W. A. Baan, RFI Mitigation Methods in Radio Astronomy, *Journal of Astronomy and Astrophysics*, Vol. 378, 2001, pp. 327-344.
- [24] S. Y. Li, E. Ali, & Z. W. Sun, RF Mitigation Researches and Implements in Radio Astronomy, *Proc. IEEE Congress on Image and Signal Processing*, Vol. 4, 2008, pp. 469-472.
- [25] ETA Project Website, [Online]. Available: <http://www.ece.vt.edu/swe/eta>
- [26] S. Uda, Wireless Beam of Short Electric Waves, *Journal of IEE (Japan)*, 1926, pp. 273-282, and 1927, pp. 1209-1219.
- [27] H. Yagi, Beam Transmission of Ultra Short Waves, *Proc. IRE*, Vol. 16, 1928, pp. 715-741.
- [28] J. D. Kraus, *Antennas* 2<sup>nd</sup> ed., New York: McGraw-Hill, 1988.
- [29] J. J. Car, *Practical Antenna Handbook* 4<sup>th</sup> ed., New York: McGraw-Hill, 2001.
- [30] R. D. Straw, and G. L. Hall, *Antenna Height and Communications Effectiveness* 2<sup>nd</sup> ed., The American Radio Relay League, Inc., 1999.